

## Estimation of hyporheic water residence time in situ using $^{222}\text{Rn}$ disequilibrium

Sébastien Lamontagne\* and Peter G. Cook

CSIRO Land and Water, PMB 2 Glen Osmond SA 5064, Australia

### Abstract

Radon-222 is a naturally occurring radioactive gas (half-life = 3.8 d) that is emitted by virtually all geologic materials. Stream sediment porewater tends to approach an equilibrium  $^{222}\text{Rn}$  activity determined by the  $^{222}\text{Rn}$  production rate of the sediments and radon half-life. However, this equilibrium may not be reached when porewaters are diluted with low  $^{222}\text{Rn}$  surface waters by hyporheic exchange. Thus, the hyporheic water residence time ( $t_h$ ) can be estimated in situ based on the difference in measured hyporheic  $^{222}\text{Rn}$  activity relative to  $^{222}\text{Rn}$  activity in the absence of hyporheic exchange. To validate  $^{222}\text{Rn}$ -derived  $t_h$  estimates, a pulse in-stream bromide injection and a continuous in-stream injection of sulfur hexafluoride ( $\text{SF}_6$ ) were made in a subtropical stream (Swamp Oak Creek, Australia) along a reach with a sand, gravel, and cobble streambed. The bromide injection estimated  $t_h$  indirectly from the shape of upstream and downstream in-stream breakthrough curves, whereas the  $\text{SF}_6$  injection estimated  $t_h$  directly by the determination of hyporheic breakthrough curves. The average  $t_h$  obtained with  $^{222}\text{Rn}$  disequilibrium ( $0.095 \pm 0.086$  d;  $\pm$  SD) was similar to that obtained using bromide injection ( $0.10 \pm 0.026$  d) and within the range estimated from  $\text{SF}_6$  injection (0.05–0.2 d). Unlike the commonly used in-stream breakthrough curves of injected tracers, the  $^{222}\text{Rn}$  disequilibrium technique is advantageous because it measures  $t_h$  of transient storage for the hyporheic zone only. The  $^{222}\text{Rn}$  disequilibrium technique is only applicable to estimate  $t_h$  in the range of hours to days, but this is the range of interest in many hyporheic studies.

Pressure gradients generated by the movement of stream water over irregular streambeds induce stream water to move in and out of the streambed (Thibodeaux and Boyle 1987; Hutchinson and Webster 1998), a process also known as hyporheic exchange (Harvey and Wagner 2000). Hyporheic exchange plays an important role in solute transport, nutrient cycling, and contaminant attenuation in streams (Boulton 2000; Jones and Mullholland 2000). However, quantifying the rate of this exchange, particularly in larger streams and rivers, remains a challenge (Hinkle et al. 2000; Stanley and Jones 2000; Runkel et al. 2003). In-stream tracer injection combined with modeling of breakthrough curves is the most widely used approach to quantify hyporheic exchange in small streams

(Stream Solute Workshop 1990; Wagner and Harvey 1997). However, the use of dissolved salts as tracers is logistically complicated in larger streams and rivers because of the large volume of solution that must be used. In addition, injected tracer experiments estimate the exchange between streams and both hyporheic and surface storage zones (sluggish side pools, etc.) and are an indirect method to estimate hyporheic exchange because of the large number of parameters that must be fitted to model breakthrough curves (Runkel 1998).

An alternative to in-stream injections would be to measure hyporheic exchange in situ using naturally-occurring tracers. Radon-222 is an inert gas with a half-life of 3.8 d that is produced by the radioactive decay of radium-226, one of the members of the uranium-238 decay series. Virtually all geologic materials produce at least small quantities of  $^{222}\text{Rn}$ , and it is a commonly used tracer for identifying locations of groundwater discharge to streams (Ellins et al. 1990; Lee and Hollyday 1993; Genereux et al. 1993; Cook et al. 2003). The sources of  $^{222}\text{Rn}$  to porewater or groundwater include decay of  $^{226}\text{Ra}$  sorbed on surfaces, diffusion of  $^{222}\text{Rn}$  generated within mineral matrices, and the expulsion of  $^{222}\text{Rn}$  from mineral matrices by the  $\alpha$ -recoil process (Cecil and Green 1999). Radon-222 activity in surface water tends to be much lower

\*E-mail:sebastien.lamontagne@csiro.au; phone:+ 61-8-8303-8713;  
fax:+ 61-8-8303-8750

### Acknowledgments

This study was funded by Land & Water Australia, New South Wales Department of Infrastructure, Planning and Natural Resources, and CSIRO Land and Water. We thank Dawit Berhane, Peter Sinclair, and Michael Williams for their support during this study. Ian Webster, David Rassam, Andrew Herczeg, and two anonymous reviewers provided useful comments on earlier drafts of the manuscript.

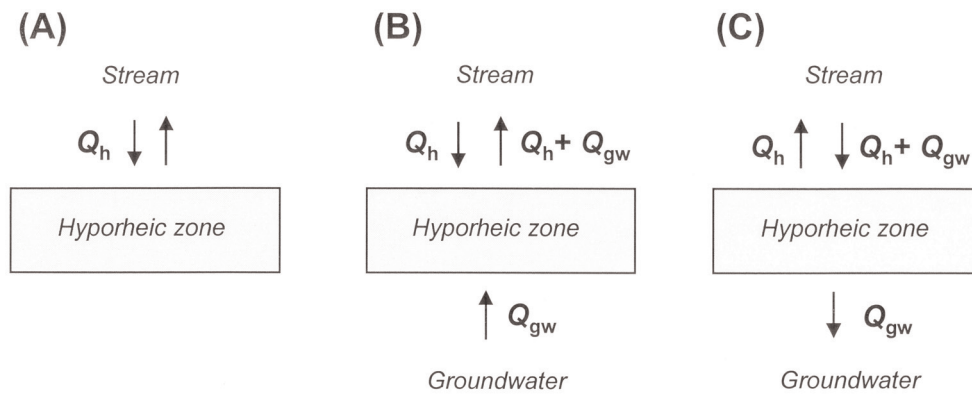


**Fig. 1.** Conceptual representation of the hyporheic zone hydrological mass-balance for different stream-reach types. (A) without groundwater recharge or discharge, (B) gaining stream, (C) losing stream.  $Q_h$  = hyporheic flux,  $Q_{gw}$  = groundwater flux.

than in pore or groundwater because of low dissolved  $^{226}\text{Ra}$  concentrations in freshwater, the short half-life of  $^{222}\text{Rn}$ , and the volatilization of  $^{222}\text{Rn}$  to the atmosphere (Cook et al. 2006). Because of its relatively short half-life, streambed porewater  $^{222}\text{Rn}$  activity should rapidly reach steady-state with its parent  $^{226}\text{Ra}$  in sediments. However, if hyporheic exchange occurs, steady-state activity will be less than expected because of dilution by low  $^{222}\text{Rn}$  activity surface water. This discrepancy between the expected and measured  $^{222}\text{Rn}$  activity in stream sediment porewater can be used to estimate the hyporheic water residence time ( $t_h$ ).

In the following, the theory for the  $^{222}\text{Rn}$  activity disequilibrium technique is described and tested in a subtropical stream (Swamp Oak Creek, New South Wales, Australia). The technique was also compared to independent estimates of  $t_h$  obtained using a bromide ( $\text{Br}^-$ ) pulse injection and a continuous injection of the inert gas sulfur hexafluoride ( $\text{SF}_6$ ). The  $\text{Br}^-$  injection estimated  $t_h$  indirectly by comparing the in-stream breakthrough curves between upstream and downstream stations, while the continuous  $\text{SF}_6$  injection measured  $t_h$  directly by comparing surface and hyporheic breakthrough curves. The practical applications, potential limitations, and further improvements to the  $^{222}\text{Rn}$  disequilibrium technique are discussed.

**Rn-222 disequilibrium theory**—We represent the hyporheic zone as a layer of constant depth beneath the stream bed, with a uniform solute concentration  $c_h$ . For the case when there is no groundwater discharge or recharge (Fig. 1a), the solute mass balance within the hyporheic zone can be expressed as

$$wh\theta \frac{dc_h}{dt} = Q_h c - Q_h c_h + \gamma wh\theta - \lambda wh\theta c_h \quad (1).$$

where  $c$  and  $c_h$  are the radon activities within the river and the hyporheic zone respectively,  $Q_h$  is the flux of water into and out of the sediments ( $\text{m}^3 \text{m}^{-1} \text{d}^{-1}$ ),  $\gamma$  is the production rate within the hyporheic zone ( $\text{Bq} \text{d}^{-1}$ ),  $h$  is the mean depth of the hyporheic zone (m),  $\theta$  is its porosity,  $w$  is the river width (m), and  $\lambda$  is the decay coefficient for radon ( $\text{d}^{-1}$ ). The assumptions of this model are that (i) the diffusive flux of Rn from the streambed is negligible relative to the advective flux; (ii)

exchange occurs in the vertical plane only (i.e., no lateral exchange); and (iii) downstream transport within the hyporheic zone is negligible.

At steady-state, the concentration within the hyporheic zone is then given by re-arrangement of Eq. 1:

$$c_h = \frac{Q_h c + \gamma wh\theta}{Q_h + \lambda wh\theta} \quad (2).$$

The average residence time of water within the hyporheic zone,  $t_h$ , is given by

$$t_h = \frac{wh\theta}{Q_h} \quad (3).$$

Substitution of Eq. 3 into Eq. 2 gives

$$c_h = \frac{c + \gamma t_h}{1 + \lambda t_h} \quad (4).$$

Thus, the radon activity within the hyporheic zone is only a function of the  $^{222}\text{Rn}$  activity in the river, the radon production rate, and the hyporheic zone water residence time. Rearranging Eq. 4,

$$t_h = \frac{c - c_h}{\lambda c_h - \gamma} \quad (5).$$

The significance of Eq. 5 is that  $t_h$ , a parameter difficult to measure in the field, can be estimated from  $c$ ,  $c_h$ , and  $\gamma$ , which are relatively easy to measure.

**Range in applicable  $t_h$** —The time range of applicability of the method is determined by the half-life of  $^{222}\text{Rn}$  and the sampling and counting errors of the radon activity measurements. Under most conditions, the upper limit in  $t_h$  that could be estimated would be  $\sim 20$  d (Fig. 2). This occurs because hyporheic water  $^{222}\text{Rn}$  activity will not change appreciably once  $t_h$  is long enough to approach steady-state with the mineral phase. However, because of inevitable measurement errors in  $c$ ,  $c_h$ , and  $\gamma$ , the error on  $t_h$  will increase when  $t_h$  will approach 20 d (a method is proposed in *Estimation of confidence intervals* below to evaluate the error and the detection limits for  $t_h$  based on  $c$ ,  $c_h$ , and  $\gamma$  measurement errors). The practical lower limit in measurable  $t_h$  will occur when  $t_h$  is too short to significantly enrich hyporheic water in  $^{222}\text{Rn}$  relative to measurement error. This lower detection

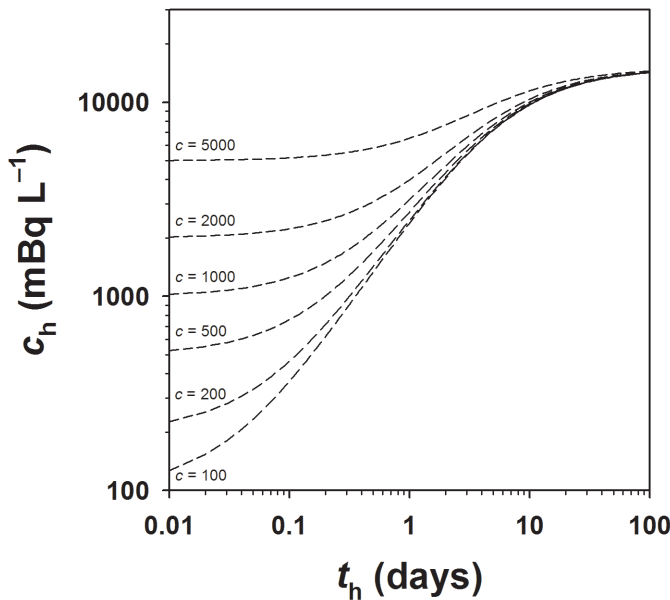


**Fig. 2.** Theoretical variation in radon activity within the hyporheic zone as a function of hyporheic water residence time and surface water radon activity ( $c$  in  $\text{mBq L}^{-1}$ ). The figure is for the case when  $\gamma/\lambda = 15,000 \text{ mBq L}^{-1}$ , a representative value for Swamp Oak Creek.

limit will tend to decrease at lower surface water  $^{222}\text{Rn}$  activities. For example, at our study site (where  $\gamma/\lambda \sim 15,000 \text{ mBq L}^{-1}$ ), the practical lower detection limit for  $t_h$  will be  $\sim 0.5 \text{ d}$  at  $c = 5000 \text{ mBq L}^{-1}$  but less than  $0.01 \text{ day}$  at  $c = 100 \text{ mBq L}^{-1}$  (Fig. 2). However, as for the case of the upper detection limit, the precision of the  $t_h$  estimates decreases when approaching the lower detection limit. Overall, the  $^{222}\text{Rn}$  disequilibrium technique is applicable over the range in  $t_h$  that is often of interest in hyporheic studies (hours to days).

**$^{222}\text{Rn}$  disequilibrium in cases with groundwater recharge or discharge**—In many natural settings the hyporheic flux to the streambed will be much larger than the groundwater flux, and Eq. 5 can be used as a first approximation to estimate  $t_h$ . However, the hyporheic zone solute mass-balance can be modified to include the flux of  $^{222}\text{Rn}$  in or out of the hyporheic zone due to the groundwater flux. The case for groundwater discharge (that is, gaining stream reaches; Fig. 1b) is probably more important because regional groundwater can be enriched in  $^{222}\text{Rn}$  and thus represent a significant flux of  $^{222}\text{Rn}$  even if a small flux of water (Cook et al. 2006). Assuming that groundwater discharge mixes uniformly with surface water in the hyporheic zone, the mass-balance for  $^{222}\text{Rn}$  becomes

$$wh\theta \frac{dc_h}{dt} = Q_h c - Q_h c_h + Q_{gw} c_{gw} - Q_{gw} c_h + \gamma wh\theta - \lambda wh\theta c_h \quad (6)$$

where  $Q_{gw}$  is the flux of groundwater, and  $c_{gw}$  is the activity of radon in groundwater. Note that, in this case, the hyporheic and groundwater fluxes out of the hyporheic zone are indistinguishable, and the definition of the hyporheic water residence time is

$$t_h^* = \frac{wh\theta}{Q_{gw} + Q_h} \quad (7).$$

(Thus, for the case with groundwater discharge,  $t_h$  as defined in Eq. 3 is the “residence time of surface water in the hyporheic zone”). At steady-state,  $t_h^*$  is

$$t_h^* = \frac{ac - c_h + c_{gw}(1 - a)}{\lambda c_h - \gamma} \quad (8)$$

where

$$a = \frac{Q_h}{Q_h + Q_{gw}} \quad (9).$$

When  $a$  is not known, there is not a unique solution to  $t_h^*$  for a given  $c_h$  (practical approaches to independently estimate  $a$  will be demonstrated in *Discussion*). However, the upper boundary can be estimated when assuming that  $a = 1$ .

The steady-state solution for the case with regional groundwater recharge (that is, losing stream reaches; Fig. 1c) is

$$t_h^* = \frac{c - c_h}{\lambda c_h - \gamma} \quad (10),$$

which is apparently similar to Eq. 5, with the exception that Eq. 10 estimates the hyporheic water residence time considering both the export of hyporheic water to the stream and to the underlying aquifer. However, in the case for groundwater recharge, the distinction between  $t_h$  and  $t_h^*$  will only be useful for the case of rapidly losing streams. In most losing streams,  $t_h \sim t_h^*$ .

**Theory for the independent estimation of  $t_h$  using in-stream injections**—A pulse in-stream injection of  $\text{Br}^-$  was used to independently estimate a stream-reach  $t_h$ . The theory behind this approach has been described in detail elsewhere (Harvey and Wagner 2000; Packman and Bencala 2000). Briefly, the hyporheic water residence time can be estimated from in-stream tracer injections using the one dimensional advection-dispersion equation combined with a transient storage model:

$$\frac{\partial c}{\partial t} + \frac{Q}{A} \frac{\partial c}{\partial x} = \frac{1}{A} \frac{\partial}{\partial x} \left( AD \frac{\partial c}{\partial x} \right) + \frac{q_L}{A} (c_L - c) + \alpha (c_s - c), \quad (11)$$

$$\frac{\partial}{\partial t} c_s = -\alpha \frac{A}{A_s} (c_s - c), \quad (12)$$

where  $c$ ,  $c_s$  and  $c_L$  are the solute concentrations in the stream, the storage zone and in lateral inflow, respectively ( $\text{M L}^{-3}$ ;  $\text{M}$ ,  $\text{L}$  – arbitrary mass and length units, respectively);  $Q$  is the volumetric flow rate in the stream ( $\text{L}^3 \text{ T}^{-1}$ ;  $\text{T}$  – arbitrary time unit);  $D$  is the dispersion coefficient ( $\text{L}^2 \text{ T}^{-1}$ );  $A$  and  $A_s$  are the cross-sectional area of the stream and the storage zone ( $\text{L}^2$ ), respectively;  $q_L$  is the lateral inflow rate ( $\text{L}^3 \text{ T}^{-1} \text{ L}^{-1}$ ; including both surface and groundwater);  $\alpha$  is the storage exchange coefficient ( $\text{T}^{-1}$ );  $t$  is time ( $\text{T}$ ); and  $x$  is the distance along the stream channel ( $\text{L}$ ). The parameters for Eqs. 11 and 12, for a particular stream reach, can be estimated by fitting theoretical tracer breakthrough curves to the ones observed during injection experiments. The hyporheic water residence time can be estimated from the transport parameters using (Harvey and Wagner 2000):

$$t_h = \frac{A_s}{\alpha A} \quad (13).$$

Theory to estimate  $t_h$  using hyporheic breakthrough curves—Hyporheic breakthrough curves observed during a continuous in-stream injection of the inert gas  $\text{SF}_6$  were used as another independent approach to estimate  $t_h$ .  $\text{SF}_6$  was chosen instead of  $\text{Br}^-$  for this experiment because of the relative ease to label large volumes of water for longer periods of times with dissolved gases. By removing the production and decay terms, the mass-balance models developed for  $^{222}\text{Rn}$  (Eqs. 1 and 6) can also be used to estimate  $t_h$  from  $\text{SF}_6$  hyporheic breakthrough curves. For the case without groundwater discharge or recharge, the mass-balance for inert tracers becomes

$$\frac{dc_h}{dt} = \frac{(c - c_h)}{t_h} \quad (14).$$

Assuming that  $c_{\text{gw}} = 0$ , for gaining stream reaches, the mass-balance becomes

$$\frac{dc_h}{dt} = \frac{(ac - c_h)}{t_h^*} \quad (15),$$

and for losing stream reaches, it becomes

$$\frac{dc_h}{dt} = \frac{(c - c_h)}{t_h^*} \quad (16).$$

Analytical solutions are available for Eqs. 14–16 for simple boundary condition problems (Lamontagne and Cook, unpubl. data), and simple numerical approximations can be used for more complex boundary conditions. Because the input boundary condition for the models is the observed surface water  $\text{SF}_6$  concentration over time at the point of hyporheic sampling, loss of  $\text{SF}_6$  to the atmosphere between the location of  $\text{SF}_6$  injection and the sampling points does not need to be quantified.

## Materials and procedures

*Sampling for hyporheic and surface water  $^{222}\text{Rn}$* —A range of drivepoints and mini-piezometers have been developed to sample hyporheic water (Boulton 1993; Duff et al. 1998). In this study, we used mini-piezometer nests made of 6 mm outer diameter by 4 mm inner diameter nylon tubing, with their bottom ends screened with fine mesh cloth, and fastened in pairs of different lengths to 5 mm dia. wooden rods. The minipiezometer nests were installed using a technique similar to the one outlined in Boulton (1993). Briefly, casings (20 mm outer diameter polyvinyl chloride) were first installed in the streambed down to one meter, or as far as practical, using a percussion technique (Boulton 1993). The mini-piezometer nests were then inserted within the casings, and the casings gently removed while the nests were held in place using the wooden rods. The combination of purging (two piezometer volumes) and collection of the  $^{222}\text{Rn}$  samples removed 20 to 29 mL of hyporheic water for a 30 cm and 100 cm minipiezometer, respectively. Assuming a porosity of  $\sim 0.4$  in a sand, gravel, and cobble hyporheic zone (Freeze and Cherry 1979) and an isotropic porous medium, the volume of hyporheic zone sampled would represent a sphere with a radius of  $\sim 2.5$  cm for the shorter piezometers and  $\sim 2.7$  cm for the longer piezometers. Thus, the volume of hyporheic water sampled with this design will be relatively small when the

average length scale of hyporheic processes will be in the tens of centimeters to meter range, as expected in sand, gravel, and cobble streambeds (Jones and Mulholland 2000).

To avoid degassing of  $^{222}\text{Rn}$ , special care must be taken not to expose hyporheic water samples to the atmosphere. Hyporheic water was pumped from minipiezometers using a hand-operated peristaltic pump. Following purging of the piezometers and while gentle pumping continued, 14 mL of hyporheic water was collected without exposure to the atmosphere by completely inserting the needle of a glass syringe inside the open end of the pump tubing. The sample was then immediately injected into a pre-weighed 22 mm Teflon-coated PTFE scintillation vial containing 6 mL Packard NEN mineral oil, taking care to keep the end of the needle below the mineral oil surface. Radon activity was counted in the laboratory by liquid scintillation, on a LKB Wallac Quantulus counter using the pulse shape analysis program to discriminate  $\alpha$  and  $\beta$  decay (Herczeg et al. 1994).

For surface water  $^{222}\text{Rn}$ , larger sample volumes are required because the radon activity can be much lower than in hyporheic water because of volatilization loss to the atmosphere. The technique used to collect and analyze surface water  $^{222}\text{Rn}$  is described in Leaney and Herczeg (2006) and will only be briefly summarized here. Surface water samples were collected in 1250 mL plastic (PET) bottles without leaving a headspace. Within 24 h of collection,  $^{222}\text{Rn}$  was extracted by first discarding  $\sim 50$  mL of water and by adding 20 mL of mineral oil scintillant from a pre-weighed scintillation vial. The bottle was then capped and shaken for 4 min to equilibrate the radon between the air-water-scintillant phases. After allowing the scintillant to settle at the top of the bottle (about 1 min), the scintillant was returned to the vial and sealed. Efficiency of radon extraction and counting was approximately 50%, and duplicates were within 5%.

*$^{222}\text{Rn}$  production rate*—Measurements of radon production rate were made on sediments collected from the streambed. Approximately  $\sim 40$  g of oven-dried sediment were sealed in 60 mL brass containers, with 20 mL of mineral oil scintillant. The balance of the volume ( $\sim 20$  mL) was filled with distilled water. After a period of several weeks, the radon activity within the chamber will reach a constant value as the radon production rate from the sediment will be exactly balanced by the radon loss due to radioactive decay. After allowing 6 weeks for steady-state porewater  $^{222}\text{Rn}$  activity to be reached, the mineral oil was sampled, and its radon concentration was measured. By using a series of  $^{226}\text{Ra}$  standard solutions with different activities (derived from dilutions of the  $^{226}\text{RaCl}_2$  SRM 4950E standard from the National Institute for Science and Technology), the efficiency of this process (percentage of emanated radon that is captured in the scintillant) was determined to be approximately 61%. The radon activity in the mineral oil is used to calculate the total radon emanation,  $E$  ( $\text{Bq kg}^{-1}$ ), which is related to the radon production rate,  $\gamma$  ( $\text{Bq L}^{-1} \text{d}^{-1}$ ) by

$$\gamma = \frac{E(1 - \theta)\rho_s\lambda}{\theta} \quad (17)$$

where  $\rho_s$  is the density of the solid phase.

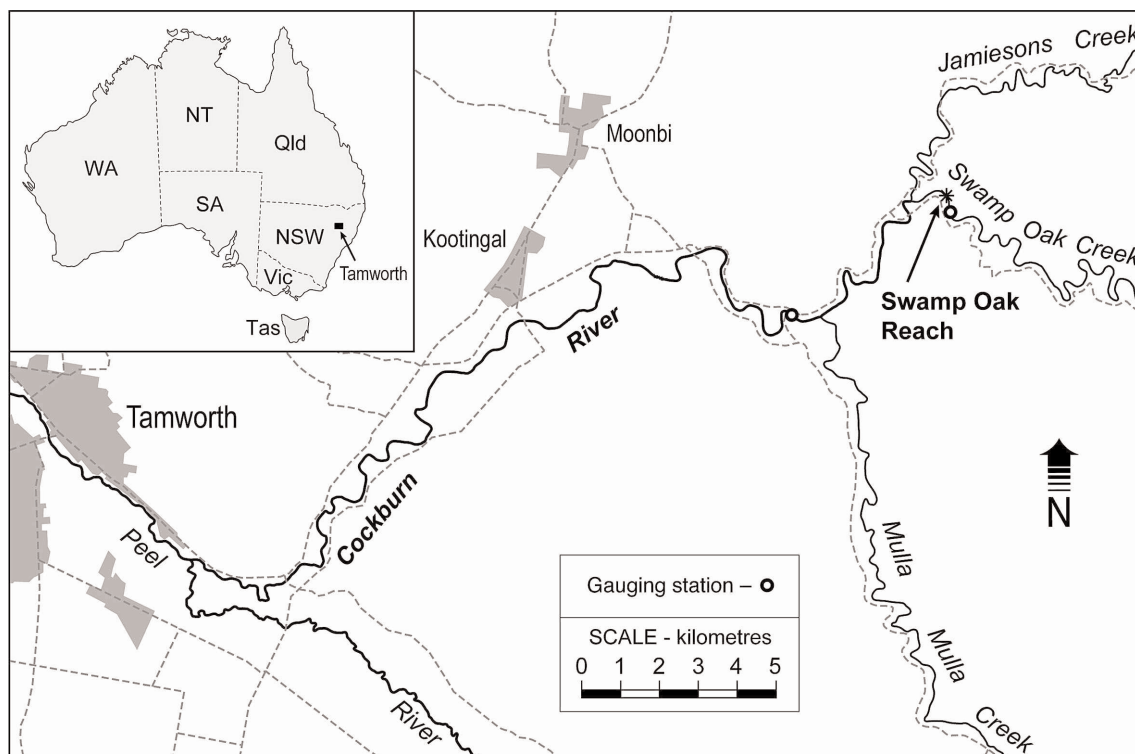


**Fig. 3.** Location of Swamp Oak Creek (New South Wales) and the experimental study reach.

*Estimation of confidence intervals*—Confidence intervals for  $t_h$  estimated with  $^{222}\text{Rn}$  disequilibrium will be a combination of the sampling and measurement errors on  $c$ ,  $c_h$ , and  $\gamma$  (Eq. 5). Estimating the error on  $t_h$  is especially important when  $c \sim c_h$  because  $t_h$  is calculated in part from the difference between the two values (Eq. 5). Because the underlying error distribution for  $c$ ,  $c_h$ , and  $\gamma$  may not be known, permutation tests (which are insensitive to the underlying error distribution) can be used to estimate  $t_h$  confidence intervals (Manly 1997). The error on  $t_h$  from individual piezometer samples and for the average from all piezometers used at the study reach were estimated with bootstrap tests (Manly 1997). Essentially, a bootstrap test generates a distribution of  $t_h$  estimates (10,000 here), which are derived by generating “new” mean  $c$ ,  $c_h$ , and  $\gamma$  values for each iteration by random permutation (with replacement) of the original  $c$ ,  $c_h$ , and  $\gamma$  data sets. See Manly (1997) for a detailed treatment on how to use bootstrap tests to estimate confidence intervals. A slightly different approach was taken to estimate the  $t_h$  confidence intervals from individual piezometers because only one  $c_h$  value was available for each of them. In this case, a random  $c_h$  value was calculated for each iteration of the bootstrap test by assuming that the error on  $c_h$  followed a normal distribution with a standard deviation equal to 10% of the mean (twice the  $^{222}\text{Rn}$  activity measurement error). The 95% confidence intervals for  $t_h$  can be estimated by using the 2.5 and 97.5 percentile from the bootstrap distributions.

### Assessment

*Study site*—Swamp Oak Creek is one of the major tributaries of the Cockburn River, Australia (Fig. 3). The majority of the Cockburn catchment is part of the New England Fold belt and consists of a Cambrian to Silurian ophiolitic sequence, which was uplifted and subjected to mild metamorphism in the Late Carboniferous. In the late Permian, the sediments were intruded by the New England Batholith (granite), which underlies the Cockburn River. Climate in the region is subtropical, with long, hot summers and cool winters. Mean annual precipitation at Tamworth is 670 mm and is relatively evenly distributed throughout the year. The study reach was the 300 m section downstream from the Swamp Oak Creek gauging station (Fig. 3). This section of Swamp Oak Creek has a shallow (10 – 100 cm) coarse sand, gravel, and cobble stream bed overlying bedrock and a baseflow of approximately  $0.08 \text{ m}^3 \text{ s}^{-1}$ . The channel width along the study reach varied between 4.6 and 15 m (Table 1).

Two mini-piezometer nests were installed in Swamp Oak Creek on 12 October 2005 (Table 1). The nests were installed 200 m downstream from the point of  $\text{SF}_6$  injection and also corresponded to Station 2 of the  $\text{Br}$  injection experiment (see details below). Hyporheic  $^{222}\text{Rn}$  activity was sampled on 13 October 2005, a period when stream flow was constant (Fig. 4).

*$^{222}\text{Rn}$ -derived  $t_h$* —Surface water  $^{222}\text{Rn}$  activity was  $426 \pm 48.7 \text{ mBq L}^{-1}$  (mean  $\pm$  SD,  $n = 8$ ) at Swamp Oak between 13 –

**Table 1.** Details of mini-piezometers installed at Swamp Oak Creek, with range in width and wetted perimeter from three nearby cross-sections.

Width (m)	Wetted perimeter (m)	Q (m <sup>3</sup> s <sup>-1</sup> )	Mini-piezometer	Depth below stream bed (cm)	Water depth (cm)	Stream velocity (m s <sup>-1</sup> )
4.6 – 15	0.35 – 1.4	0.085	MP1-S	35	30	0.06
			MP1-D	75		
			MP2-S	30	30	
			MP2-D	60	60	

18 October 2005 (Table 2) while hyporheic <sup>222</sup>Rn activities ranged between 420 to 950 mBq L<sup>-1</sup> between mini-piezometers (Table 3). Cook et al. (2006) determined that radon production rates were 2480 ± 640 mBq L<sup>-1</sup> d<sup>-1</sup> (mean ± SD) in sediments from Swamp Oak (Table 2), similar to values found in nearby Cockburn River sediments (2790 ± 840 mBq L<sup>-1</sup> d<sup>-1</sup>). Hyporheic water residence times derived from individual piezometers ranged between < 0.035 and 0.23 d, with an average of 0.095 ± 0.086 day when combining values from all mini-piezometers (Table 3).

The measured hyporheic <sup>222</sup>Rn activity at MP2S was slightly smaller (420 mBq L<sup>-1</sup>) than the average surface water <sup>222</sup>Rn activity (426 ± 48.7 mBq L<sup>-1</sup>). This probably represents a case where hyporheic exchange was rapid (yielding  $c \sim c_h$ ) and where  $c > c_h$  because of measurement error. In such cases, the 97.5 percentile  $t_h$  obtained from the bootstrapped  $t_h$  distribution can be used to set an upper detection limit for  $t_h$ . For example, piezometer MP2S had a mean  $t_h = -0.0022$  d and a 97.5 percentile  $t_h = 0.035$  d, suggesting that  $t_h$  is < 0.035 d (Table 3; Fig. 5). To yield precise estimates of  $t_h$ , special care should be taken when measuring  $c$  and  $c_h$  when  $c \sim c_h$ .

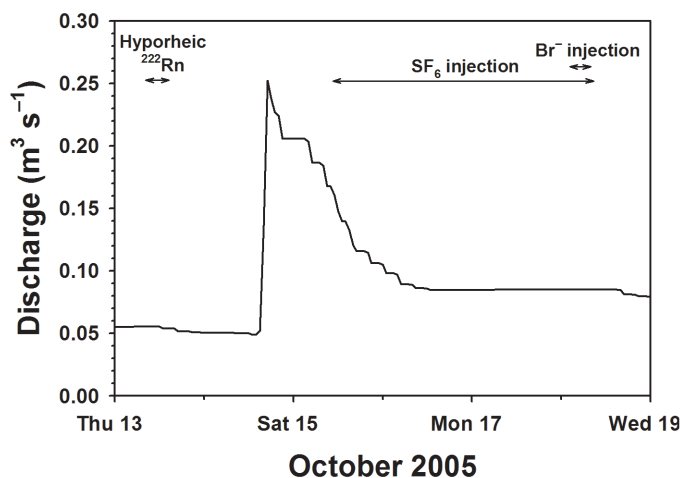
**Bromide injection experiment**—A bromide pulse injection was carried out at Swamp Oak on 18 October 2005 to estimate  $t_h$  using in-stream breakthrough curves. An inflatable swimming pool was filled with 40 L bromide brine (~1.13 kg L<sup>-1</sup>) that was injected in the stream using a peristaltic pump connected to a

spraying system designed to release the brine over most of the stream width. Downstream sampling stations were set up 110 m (Station 1) and 295 m (Station 2) from the point of injection. Brine was injected in the stream for 40 min, at which time the injection was stopped (with ~38.4 L injected). Sampling occurred at the downstream stations at 1 to 4 min intervals, with a higher sampling frequency when the bromide pulse was detected (as assessed by simultaneous electrical conductivity measurements). Water samples were collected mid-stream using 125 mL polyethylene bottles. Sampling proceeded until 150 min after the injection was started. Stream discharge was 0.085 m<sup>3</sup> s<sup>-1</sup> and remained constant throughout the injection. Bromide concentrations were measured by ion chromatography.

The model OTIS-P was used to estimate the parameters of Eqs. 11 and 12 from the Br<sup>-</sup> injection. Model details can be found in Runkel (1998). Briefly, OTIS-P provides numerical solutions for advective-dispersive transport with transient storage under a variety of conditions (steady or unsteady flow, pulse or continuous injection, etc.) and includes sub-routines for parameter optimization. The observed Br<sup>-</sup> concentration curve at Station 1 was used as the input function for the tracer. The best fit for the Br<sup>-</sup> breakthrough curve at Station 2 was estimated by allowing the model to optimize the values for  $D$ ,  $A$ ,  $A_s$ , and  $\alpha$ . Stream discharge was set at 0.085 m<sup>3</sup> s<sup>-1</sup>, and it was assumed that lateral inflow of groundwater and surface water was negligible ( $q_L = 0$ ) between stations 1 and 2 (consistent with observations in Cook et al. [2006]).

**Table 2.** Stream <sup>222</sup>Rn activity ( $c$ ) measured at Swamp Oak Creek between 13–18 October 2005 and <sup>222</sup>Rn production rate in sediments ( $\gamma$ ) measured at Swamp Oak Creek and in the Cockburn River (Station 15.6 km in Cook et al. [2006]).

$c$ (mBq L <sup>-1</sup> )	$\gamma$ (mBq L <sup>-1</sup> d <sup>-1</sup> )	
	Swamp Oak	Cockburn
410	2790	3960
450	2270	2350
490	3150	2790
460	1690	2050
330		
420		
450		
400		

**Fig. 4.** Hydrograph for Swamp Oak Creek, 13–19 October 2005. The approximate periods when the measurements of hyporheic <sup>222</sup>Rn, the injection of SF<sub>6</sub>, and the injection of Br<sup>-</sup> were made are indicated.

**Table 3.** Hyporheic water residence times estimated using <sup>222</sup>Rn disequilibrium

Piezometer	$c_h$ (mBq L <sup>-1</sup> )	Mean $t_h$ (d)	Median $t_h$ (d)	SD (d)	P(2.5%) (d)	P(97.5%) (d)
Per individual piezometer						
MP1D	660	0.101	0.099	0.033	0.042	0.169
MP1S	560	0.058	0.057	0.027	0.009	0.113
MP2D	950	0.232	0.228	0.053	0.138	0.346
MP2S	420	-0.002	-0.002	0.019	-0.040	0.0351
Combining all piezometers						
All		0.095	0.078	0.086	-0.012	0.268

All statistics estimated using a bootstrap test. When a mean negative  $t_h$  was estimated the upper 97.5 percentile can be used to set the upper detection limit.

The peaks in the Br<sup>-</sup> concentration occurred at 49 and 80 min at stations 1 and 2, respectively, and were both characterized by trailing tails indicative that exchange with a storage zone was occurring (Fig. 6). Modelling of the Station 2 breakthrough curve indicated that the storage zone for this stream section ( $A_s = 0.53$  m<sup>2</sup>) was approximately half that of the stream cross-sectional area ( $A = 0.97$  m<sup>2</sup>; Table 4). While the optimized fit for all four parameters gave a good match between the observed and predicted Br<sup>-</sup> curves, it was felt that a better fit could be made for the tail end (a part of the curve strongly influenced by exchange with a storage zone; Harvey and Wagner 2000). Thus, additional OTIS-P runs were made for fixed  $\alpha$  values while the remaining three parameters ( $A$ ,  $A_s$ , and  $D$ ) were still being optimized by the model. The best fit for the tail end of the curve was for  $\alpha = 7.5 \times 10^{-5}$  s<sup>-1</sup> (Fig. 6), with minimal differences on the values of the other parameters (Table 4).

Assuming that only hyporheic exchange occurs and using Eq. 13, the average water residence time in the hyporheic zone was  $0.10 \pm 0.026$  day between stations 1 and 2.

*SF<sub>6</sub> injection experiment*—A continuous injection of SF<sub>6</sub> was carried out from 15–18 October 2005. The details of the injection have been described in Cook et al. (2006) and the key methods only briefly summarized here. A 600 mL stainless steel vessel was filled with SF<sub>6</sub> to a pressure of 623 kPa. The tank was then attached to a diffuser (25 m of 3 mm diameter silicone tubing) via a regulator that maintained the pressures in the diffuser at approximately 60 kPa. The apparatus was submerged on the bed of the river at 9:35 on October 15. The pressure in the tank was measured at regular intervals to ensure that a constant injection rate was maintained. Hyporheic zone SF<sub>6</sub> concentrations were measured using the mini-piezometer nests MP1 and MP2 at  $t = -0.2, 8, 24.5, 55,$  and 75 h after the start of injection. The sampling frequency was kept conservatively low to prevent

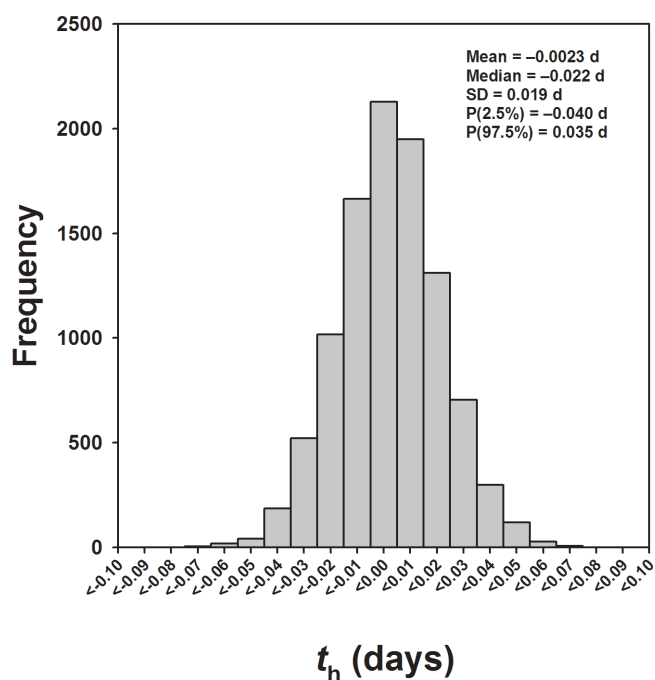


**Fig. 5.** Estimated distribution of hyporheic turnover times at MP2S using a bootstrap test.

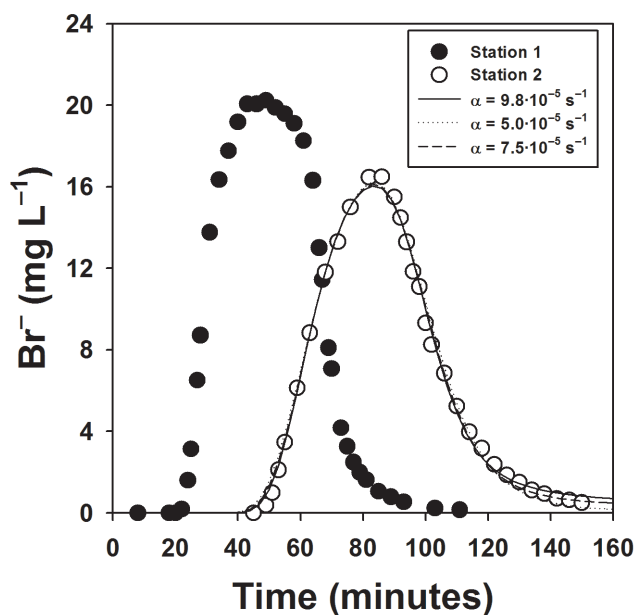


**Fig. 6.** Breakthrough curves for the Br<sup>-</sup> injection, 18 October 2005, and predicted breakthrough curves at Station 2 for different  $\alpha$  estimates.

**Table 4.** Estimated parameters for 1-dimensional advective-dispersive solute transport with transient storage for the bromide injection

	Optimized for all four parameters	With $\alpha$ constrained
$D$ (m <sup>2</sup> s <sup>-1</sup> )	0.54 ± 0.053	0.64 ± 0.036
$A$ (m <sup>2</sup> )	0.97 ± 0.013	1.0 ± 0.008
$A_s$ (m <sup>2</sup> )	0.53 ± 0.090	0.66 ± 0.17
$\alpha$ (s <sup>-1</sup> )	$9.8 \times 10^{-5} \pm 1.0 \times 10^{-5}$	$7.5 \times 10^{-5}$
$t_h$ (d)	0.065 ± 0.013	0.10 ± 0.026

The mean and standard deviation for  $D$ ,  $A$ ,  $A_s$ , and  $\alpha$  were determined using a nonlinear least-square optimization technique (Runkel 1998).  $t_h$  was estimated using Eq. 13 and the error on  $t_h$  estimated using first order error propagation (Meyer 1975).

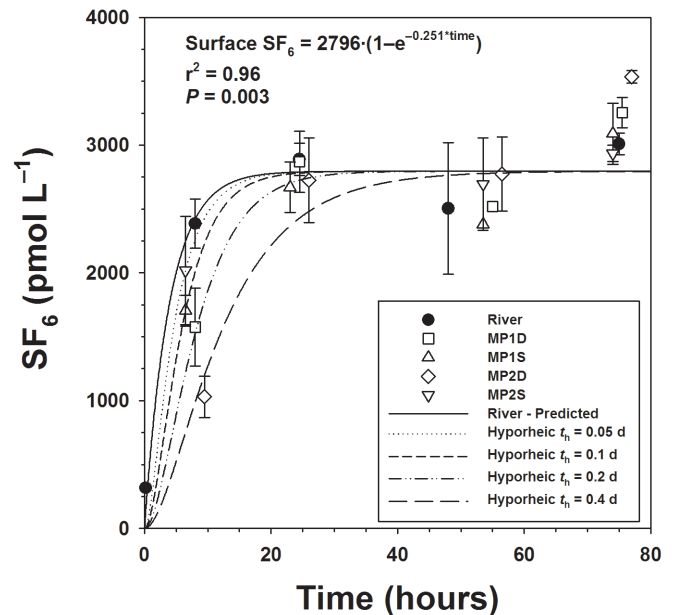
excessive entrainment of surface water to the hyporheic zone by pumping.

SF<sub>6</sub> concentration in surface water increased rapidly and concentrations varied between 2500 and 2900 pmol L<sup>-1</sup> after 24 h of injection (Cook et al. 2006). However, the change in surface water SF<sub>6</sub> concentration during the first 24 h of injection was mostly due to a decrease in stream flow during that period (less dilution of the tracer; Fig. 4) rather than the time for the SF<sub>6</sub> plume to travel 200 m downstream to MP1 and MP2 (< 1 h). SF<sub>6</sub> concentrations in MP1 and MP2 also increased rapidly but were less than surface water concentrations at  $t = 8$  h, especially in the deeper piezometers (Fig. 7). However, stream and mini-piezometer SF<sub>6</sub> concentrations were within analytical error at  $t > 8$  h.

Because of the variability in surface water SF<sub>6</sub> concentration during the first 24 h of injection, a forward difference numerical solution to Eq. 14 (Lamontagne and Cook, unpublished) was used to predict hyporheic SF<sub>6</sub> breakthrough curves for a range in  $t_h$  values. The boundary conditions for the model were (1)  $c_h = 0$  at  $t = 0$  and (2)  $c = c(t)$ , where  $c(t)$  was an exponential function fitted to the observed stream SF<sub>6</sub> concentrations (Fig. 7). The choice of an exponential function to define  $c(t)$  was arbitrary but was consistent with the expected trends in surface water SF<sub>6</sub> concentrations due to changes in stream discharge during the experiment (Fig. 4). The observed hyporheic SF<sub>6</sub> concentrations in mini-piezometers matched theoretical curves with  $t_h$  ranging from 0.05 to 0.2 d, a similar range to that observed with <sup>222</sup>Rn disequilibrium (< 0.035 to 0.23 d).

## Discussion

Overall, the  $t_h$  values measured with <sup>222</sup>Rn hyporheic disequilibrium were consistent with independent estimates of  $t_h$  obtained using tracer injections. We have also demonstrated how the method can be used to estimate the range in  $t_h$  across a stream-reach by using individual piezometer samples or a whole-reach estimate by combining several piezometer samples. The agreement between the different methods used is encouraging but should be interpreted with some caution because of two limitations of the experimental design. Firstly,

**Fig. 7.** Observed (mean ± SD) and predicted SF<sub>6</sub> hyporheic breakthrough curves for different  $t_h$  estimates.

stream velocity was not constant amongst the field experiments. Because the hyporheic flux is proportional to the square of stream velocity (Hutchinson and Webster 1998), higher stream velocities will tend to increase the hyporheic flux. This should decrease  $t_h$ , unless the size of the hyporheic zone also increases at higher stream velocities (see Eq. 13). Thus, the influence of changes in stream velocity amongst experiments on  $t_h$  is not straightforward to determine. Because there was only a ~20% difference in stream velocity between the measurement periods for hyporheic <sup>222</sup>Rn and the Br<sup>-</sup> injection, their  $t_h$  values should be comparable (Fig. 4; Note that this graph shows stream discharge and that stream velocity only increases to the cubic root of stream discharge; Leopold and Maddock [1953]). However, it is less clear how the expected variability in stream velocity during the SF<sub>6</sub> injection influenced  $t_h$  (Fig. 4). Secondly, even with a constant stream velocity, the different methods used may not necessarily yield exactly similar  $t_h$  because they may measure exchange with different types of storage zones. The Br<sup>-</sup> injection experiment measured an integrated  $t_h$  for surface and hyporheic storage zones (Runkel 1998), while the SF<sub>6</sub> injection and <sup>222</sup>Rn disequilibrium estimates were for the hyporheic zone only. However, there was no obvious surface storage zone at the study reach (sluggish side pools, etc.) and the  $t_h$  obtained from the Br<sup>-</sup> injection should approximate the one expected for the hyporheic zone only. Despite these caveats, the tracer injections supported the hypothesis that <sup>222</sup>Rn disequilibrium can be used to estimate the hyporheic water residence time.

*Hyporheic water residence time or groundwater age?*—The method proposed here to estimate  $t_h$  using <sup>222</sup>Rn is probably only valid at the scale of hyporheic exchange processes caused by the

advection of stream water over an uneven streambed (centimeters to a few meters; Harvey and Wagner 2000). A key assumption of the technique is that downstream transport within the hyporheic zone is negligible. In other words, the method can be applied when the volume of water removed from shallow piezometers “integrates” a number of hyporheic flow paths rather than collect water at one point along a distinct flowpath. Thus, the  $^{222}\text{Rn}$  disequilibrium method is probably not suitable for hyporheic exchange processes occurring at larger spatial scales (several meters to hundreds of meters) where distinct flowpaths are more likely to occur. Examples of larger scale hyporheic exchange processes include preferential downwelling and upwelling zones along pool-riffle sequences or the preferential flow of groundwater across floodplains through buried stream channels. However, the bulk volume of hyporheic exchange is thought to occur at the spatial scales covered by the  $^{222}\text{Rn}$  disequilibrium technique (Harvey and Wagner 2000).

For problems where distinct and longer flowpaths can be identified,  $^{222}\text{Rn}$  disequilibrium can be used to measure the time since recharge occurred instead (Bertin and Bourg 1994; Hoehn and Cirpka 2006). In this case, groundwater age can be estimated by using the equation describing the ingrowth of a radioactive progeny from its parent (Hoehn and von Gunten 1989):

$$A_t = A_0(1 - e^{-\lambda t}) \quad (18)$$

where  $A_t$  is the measured  $^{222}\text{Rn}$  activity in subsurface water,  $A_0$  the expected  $^{222}\text{Rn}$  activity at steady-state, and  $t$  is time since surface water entered the subsurface.  $A_0$  can be either estimated by sampling hyporheic water expected to be older than 20 d (that is, after steady-state  $^{222}\text{Rn}$  activity is achieved) or by using the radon emanation method (where  $A_0 = \gamma/\lambda$ ). A detailed development of the  $^{222}\text{Rn}$  dating method is presented in Hoehn and von Gunten (1989) and Hoehn et al. (1992). Whether  $^{222}\text{Rn}$  should be used to estimate the hyporheic water residence time or groundwater age must be determined by the experimenters based on their knowledge of the local hydrogeological environment.

*Further improvements to the technique*—The  $^{222}\text{Rn}$  disequilibrium technique still needs to be field tested for cases where the hyporheic zone is a mixture of surface and groundwater discharge. The study reach used here was not a groundwater discharge zone (Cook et al. 2006). This was also demonstrated by the  $\text{SF}_6$  injection experiment, where surface and hyporheic  $\text{SF}_6$  concentrations were similar at  $t > 8$  h, demonstrating that hyporheic water was completely derived from surface water. Stream  $\text{SF}_6$  concentrations would have been greater than hyporheic  $\text{SF}_6$  concentrations at steady-state if groundwater discharge had occurred (Triska et al. 1993).

If groundwater discharge had occurred at the Swamp Oak study reach,  $a$  would have required independent estimation to find a unique  $t_h^*$  for a given  $c_h$ . Following on Eq. 9, a unique value for  $t_h^*$  can be obtained by independently measuring  $Q_{\text{gw}}$  at a study site. Several techniques are available to determine whether or not a stream section is gaining or losing and to

determine the magnitude of  $Q_{\text{gw}}$ . Reach-scale groundwater discharge rates can be estimated using stream discharge increments between upstream and downstream stations. Changes in surface water  $^{222}\text{Rn}$  activity between upstream and downstream stations can also be used to estimate  $Q_{\text{gw}}$  (Cook et al. 2006). Alternatively, a site-specific  $Q_{\text{gw}}$  can be estimated from piezometric head differences and the hydraulic conductivity of the streambed (Lee and Cherry 1978; Boulton 1993). Sub-surface mixing between surface and groundwater can also be assessed with conservative solutes, such as chloride, using end-member mixing analysis (Bertin and Bourg 1994).

Another option is to combine  $^{222}\text{Rn}$  disequilibrium measurements with the observation of hyporheic breakthrough curves during continuous in-stream injections of inert tracers. At steady-state and for an inert tracer, it can be demonstrated that the hyporheic zone mass-balance (Eq. 6) simplifies to:

$$a = \frac{Q_h}{Q_{\text{gw}} + Q_h} = \frac{c_h^o}{c^o} \quad (19),$$

where  $c_h^o$  and  $c^o$  are the steady-state tracer concentration in the hyporheic zone and surface water, respectively. Therefore, when  $c$  remains constant during injection experiments of a conservative tracer (no change in tracer injection rate and no change in stream discharge),  $a$  can be estimated when  $c_h$  becomes constant in the hyporheic zone. Once  $a$  is known, both  $t_h^*$  and  $t_h$  can be estimated because  $t_h^* = a \times t_h$ . Thus, two estimates of  $t_h$  can be obtained by combining the  $^{222}\text{Rn}$  disequilibrium and hyporheic breakthrough curve techniques. The use of inert gases such as  $\text{SF}_6$  appears particularly promising to describe hyporheic breakthrough curves because they are more practical to use than dissolved salts for continuous injections, especially in larger streams and rivers.

### Comments and recommendations

The  $^{222}\text{Rn}$  disequilibrium technique is a simple method to estimate the hyporheic water residence time in situ. The technique also measures hyporheic exchange only, while most injected tracer experiments measure exchange with both surface and hyporheic storage zones.  $\text{Rn-222}$  disequilibrium could be used to independently validate hyporheic water residence times estimated with injected tracers, or to gain some understanding of the variability in hyporheic exchange processes within a given study reach. The disadvantages of the  $^{222}\text{Rn}$  disequilibrium technique is that it can only measure hyporheic water residence times over a restricted range (hours to days), but this is the time-scale of interest in many studies. Future studies should look at the case with groundwater discharge and consider alternative conceptual representations of the hyporheic zone.

### References

- Bertin, C., and A. C. M. Bourg. 1994. Radon-222 and chloride as natural tracers of the infiltration of river water into an alluvial aquifer in which there is significant river/groundwater mixing. *Environ. Sci. Technol.* 28:794-798.

- Boulton, A. J. 1993. Stream ecology and surface—hyporheic hydrologic exchange: implications, techniques and limitations. *Aust. J. Mar. Freshw. Res.* 44:553-564.
- . 2000. River ecosystem health down under: Assessing ecological condition in riverine groundwater zones in Australia. *Ecosyst. Health* 6:108-118.
- Cecil, L. D., and J. R. Green. 1999. Radon-222, p. 175-194. *In* P. G. Cook and A. L. Herczeg [eds.], *Environmental tracers in subsurface hydrology*. Kluwer.
- Cook, P. G., G. Favreau, J. C. Dighton, and S. Tickell. 2003. Determining natural groundwater influx to a tropical river using radon, chlorofluorocarbons and ionic environmental tracers. *J. Hydrol.* 277:74-88.
- , S. Lamontagne, D. Berhane, and J. F. Clark. 2006. Quantifying groundwater discharge to streams using dissolved gas tracers  $^{222}\text{Rn}$  and  $\text{SF}_6$ , Cockburn River, Southeastern Australia. *Water Resour. Res.* 42:W10411, doi:10.1029/2006WR0049921.
- Duff, J. H., F. Murphy, C. C. Fuller, F. J. Triska, J. W. Harvey, and A. P. Jackman. 1998. A mini drivepoint sampler for measuring porewater solute concentrations in the hyporheic zone of sand-bottom streams. *Limnol. Oceanogr.* 43:1378-1398.
- Ellins, K. K., A. Roman-Mas, and R. Lee. 1990. Using  $^{222}\text{Rn}$  to examine groundwater/surface discharge interaction in the Rio Grande De Manati, Puerto Rico. *J. Hydrol.* 115:319-341.
- Freeze, R. A., and J. A. Cherry. 1979. *Groundwater*. Prentice-Hall.
- Geneux, D. P., H. F. Hemond, and P. J. Mulholland. 1993. Use of radon-222 and calcium as tracers in three-end-member mixing model for streamflow generation on the west fork of Walker Branch Watershed. *J. Hydrol.* 142:167-211.
- Harvey, J. W., and B. J. Wagner. 2000. Quantifying hydrologic interactions between streams and their subsurface hyporheic zones, p. 3-44. *In* J. B. Jones and P. J. Mulholland [eds.], *Streams and ground waters*. Academic.
- Herczeg, A. L., J. C. Dighton, M. L. Easterbrook, and E. Salomons. 1994. Radon-222 and Ra-226 measurements in Australian groundwaters using liquid scintillation counting, p. 53-57. *In* Proceedings of the workshop on radon and radon progeny measurements in environmental samples, February 1994, Canberra.
- Hinkle, S. R., and others. 2000. Linking hyporheic flow and nitrogen cycling near the Willamette River – a large river in Oregon, USA. *J. Hydrol.* 244:157-180.
- Hoehn, E., and O. A. Cirpka. 2006. Assessing residence times of hyporheic ground water in two alluvial flood plains of the Southern Alps using water temperature and tracers. *Hydrol. Earth Syst. Sci.* 10:553-563.
- and H. R. von Gunten. 1989. Radon in groundwater: A tool to assess infiltration from surface waters to aquifers. *Water Resour. Res.* 25:1795-1803.
- H. R. von Gunten, F. Stauffer, and T. Dracos. 1992. Radon-222 as a groundwater tracer: A laboratory study. *Environ. Sci. Technol.* 26:734-738.
- Hutchinson, P. A., and I. T. Webster. 1998. Solute uptake in aquatic sediments due to current-obstacle interactions. *J. Environ. Eng.* 124:419-426.
- Jones, J. B., and P. J. Mulholland. 2000. *Streams and ground waters*. Academic.
- Leaney, F. W., and A. L. Herczeg. 2006. A rapid field extraction method for determination of radon-222 in natural waters by liquid scintillation counting. *Limnol. Oceanogr. Methods* 4:254-259.
- Lee, D. R., and J. A. Cherry. 1978. A field exercise on groundwater flow using seepage meters and mini-piezometers. *J. Geol. Edu.* 27:6-10.
- Lee, R. W., and E. F. Hollyday. 1993. Use of radon measurements in Carters Creek, Maury County, Tennessee, to determine location and magnitude of ground-water seepage, p. 237-242. *In* L. C. S. Gundersen and R. B. Wanty [eds.], *Field studies of radon in rocks, soils, and water*. C.K. Smoley.
- Leopold, L. B., and T. Maddock. 1953. Hydraulic geometry of stream channels and some physiographic implications. *U.S. Geol. Survey Prof. Paper* 252.
- Manly, B. F. J. 1997. *Randomization, bootstrap and Monte Carlo Methods in biology*, 2nd ed. Chapman & Hall.
- Meyer, S. L. 1975. *Data analysis for scientists and engineers*. Wiley.
- Packman, A. I., and K.E. Bencala. 2000. Modelling surface-subsurface hydrologic interactions, p.45-80. *In* J. B. Jones and P. J. Mulholland [eds.], *Streams and ground waters*. Academic.
- Runkel, R. L. 1998. One-dimensional transport with inflow and storage (OTIS): A solute transport model for streams and rivers. *U.S. Geological Survey Water Resources Investigation Report* 98-4018.
- , D. M. McKnight, and H. Rajaram. 2003. Modeling hyporheic zone processes. *Adv. Water Resour.* 26:901-905.
- Stanley, E. H., and J. B. Jones. 2000. Surface-subsurface interactions: Past, present, and future, p. 405-417. *In* J. B. Jones and P. J. Mulholland [eds.], *Streams and ground waters*. Academic.
- Stream Solute Workshop. 1990. Concepts and methods for assessing solute dynamics in stream ecosystems. *J. North Am. Benthol. Soc.* 9:95-119.
- Thibodeaux, L. J., and J. D. Boyle. 1987. Bedform-generated convective transport in bottom sediment. *Nature* 325:341-343.
- Triska, F. J., J. H. Duff, and R. J. Avanzino. 1993. The role of water exchange between a stream channel and its hyporheic zone in nitrogen cycling at the terrestrial-aquatic interface. *Hydrobiologia* 251:167-184.
- Wagner, B. J., and J. W. Harvey. 1997. Experimental design for estimating parameters of rate-limited mass transfer: Analysis of stream tracer studies. *Water Resour. Res.* 33:1731-1741.

Submitted 18 September 2006

Revised 17 June 2007

Accepted 30 June 2007